Int. J. Nanosci. Nanotechnol., Vol. 13, No. 1, March. 2017, pp. 1-9

Growth of CNTs over Fe–Co/Nanometric TiO_2 Catalyst by CVD: The Effects of Catalyst Composition and Growth Temperature

Z. S. Arabshahi[1], M. Akbarzadeh Pasha[1,2]* and F. Shahi[1]

[1]Department of Solid State Physics, Faculty of Basic Science, University of Mazandaran, P. O. Box 47416-95447, Babolsar, Iran
[2]Research lab of Carbon-based nanostructures, Faculty of Basic Science, University of Mazandaran, Babolsar, Iran

(*) Corresponding author: m.akbarzadeh@umz.ac.ir
(Received: 02 March 2015 and Accepted: 17 August 2016)

Abstract

In this research carbon nanotubes were produced by chemical vapor deposition of acetylene over a mixture of iron and cobalt catalysts supported on nanometric TiO_2 and the influences of two synthesis parameters: growth temperature and catalyst composition ratio on properties of end-product carbon nanotubes were investigated. The catalytic basis was prepared by wet impregnation method with different wt% mass ratio of Fe-Co/TiO_2=20-0/80, 15-5/80, 10-10/80, 5-15/80 and 0-20/80 wt%. The nanomaterials (catalysts and carbon nanotubes) were characterized using X-ray diffraction (XRD), field emission scanning electron microscopy (FESEM), X-ray map of elemental distribution (Xmap) and Raman spectroscopy. The results confirmed that by increasing the growth temperature from 650°C to 800°C; the growth rate, the average diameter and the amount of impurities of grown carbon nanotubes increase and their length and density decrease. Furthermore, it was observed that in comparison with monometallic Fe or Co, bimetallic compositions of these metals exhibit better catalytic activity in growth of carbon nanotubes. The highest yield of carbon nanotubes possessing minimum average diameter was obtained on Fe-Co/TiO_2 catalyst with a mass ratio of 10-10/80 wt%.

Keywords: *Carbon Nanotubes, Wet Impregnation, Chemical Vapor Deposition, TiO_2 Nanopowder, Bimetallic Catalyst Composition.*

1. INRODUCTION

Carbon nanotubes (CNTs) are seamless coaxial cylinders of one or several graphene sheets denoted by single wall carbon nanotubes, SWCNTs, or Multiwall carbon nanotubes, MWCNTs [1]. Due to their remarkable mechanical, structural, electronic, electromechanical and chemical properties [2, 3], CNTs are considered to be excellent candidates for many potential applications such as nanocomposite materials, sensors and actuators, catalyst and catalyst supports, field emitters, tips for scanning probe microscopy, energy storage devices, nanoelectronics, bio-nanomaterials and nanomedicine, hydrogen storage and fuel cell [4-12]. CNTs are generally synthesized by three major methods including arc-discharge [13], laser ablation [14] and chemical vapour deposition (CVD) [15-20]. Among these, CVD has attracted much attention owing to its advantages such as simplicity, high purity, high yield, selective, scalable and cost-effective growth of CNTs [18-20]. The CVD growth of CNTs is a catalytic reaction. Researchers have shown that monometallic or bimetallic combination of iron group metals, i.e. Fe, Co and Ni or addition of other metals to them as co-catalysts including Mo, Mg, Mn, Cr and Pd can catalyze CNTs from decomposition of different hydrocarbon gases via CVD [16, 18, 19, 21-26]. It is widely reported that various parameters

comprising of the type and composition of catalyst, the preparation method and pre-treatment of catalyst, type of catalyst support or substrate, kind and flow of hydrocarbon source, the growth temperature and growth time can deeply influence the structural features of CNTs such as their diameter and length, morphology, thermal stability, crystallinity and growth yield [16, 18, 19, 24, 27-36]. Kathyayini et al. examined the catalytic activity of Fe, Co and Fe/Co supported on Ca and Mg oxides, hydroxides and carbonates in the synthesis of CNTs via thermal CVD (TCVD) [37]. The catalyst-support mixtures were prepared by wet impregnation method. Acetylene and ethylene were used as the two different carbon sources and N_2 as the carrier gas and the synthesis reactions were conducted at 700°C. They observed that irrespective of applied support, the best yield of carbon deposit was obtained for mixture of Fe and Co compared to monometallic catalysts. Furthermore they found that calcium carbonate and magnesium oxide are the best supports among the six compositions of Ca and Mg. Pudukudy et al. reported direct decomposition of methane to CO_x-free hydrogen and CNTs over SBA-15(highly ordered mesoporous silicate) supported Ni, Co and Fe based bimetallic catalysts [38]. They concluded that the SBA-15 supported bimetallic catalysts have key role on formation of open tip CNTs. This work aims to study the variation of CNTs characteristics including mean diameter, growth rate, quality and density of growth at different temperatures ranging from 650°C to 800°C by CVD of acetylene, over bimetallic Fe-Co catalysts with different mass ratios supported on nanomeric TiO_2. TiO_2 is a well-known semiconductor material and combination of CNT with TiO_2 nanoparticles may lead to new potential application in photocatalysis [39, 40].

2. MATERIALS AND METHODS

2.1. Preparation of the Catalysts

The catalyst-support mixtures were prepared by wet impregnation method [29]. 1 g of TiO_2 nanopowder (rutile, average particle size=30 nm, 99.9%purity, supplied by US NANO) was dissolved in 10 ml of distilled water and the suspension was sonicated (15min) and stirred (10 min). Then appropriate amounts of $Fe(NO_3)_3.9H_2O$ (supplied by Merck) and $Co(NO_3).6H_2O$ (supplied by Merck) with different mass ratio of catalyst/substrate (Fe-Co/TiO_2) =20-0/80wt%, 15-5/80wt%, 10-10/80wt%, 5-15/80wt% and 0-20/80wt% were dissolved in distilled water separately and impregnated onto the mentioned TiO_2 suspension gradually. The mixture was stirred and dried on a hot plate at 80°C in atmospheric pressure. Finally the product was calcinated in an oven at 500°C for 2 h and a nanosized metal-ion doped TiO_2 catalytic powder was obtained.

2.2. Preparation of Carbon nanotubes

Synthesis of CNTs was carried out by a TCVD system at atmospheric pressure in a horizontal tubular quartz reactor (length and diameter are 1200 mm and 50 mm, respectively). The precursor gas consisting of a hydrocarbon source (acetylene) and a carrier gas (argon) with composition ratio of C_2H_2/Ar = 15/150 sccm flows over the prepared catalyst at definite temperature for 15 min. For each run, 50 mg of the catalyst powder was distributed uniformly on a quartz boat and loaded directly to the middle of the quartz reactor. After the reaction, the furnace was turned off and the product was cooled down to the room temperature under argon flow. Finally the deposited materials was weighed and characterized.

2.3. Characterization methods

The following equations indicate the percentage of carbon yield and average growth rate of resulting carbon deposit in each run:

$$\text{Carbon yield} = \frac{w_2 - w_1}{w_1} \times 100 \qquad (1)$$

Ave. growth rate = $\frac{w_2 - w_1}{growth\ time}\left(\frac{mg}{min}\right)$ (2)

Where w_2 is the total mass of final product, catalyst and carbon deposit, and w_1 is the initial mass of catalyst. The morphology and microstructure of resulting catalytic powders and CNTs were characterized by Field Emission Scanning Electron Microscopy (FESEM, MIRA\\ TESCAN). To determine the crystalline structure and average size of catalyst nanoparticles, the X-ray diffraction pattern (XRD, Bruker AXS, D8- Advance, Cu–K_α, λ= 1.54 Å) was used. The approximate sizes of metal oxide particles were calculated by the Scherrer equation:

$$D = \frac{K\lambda}{\beta\ Cos\ \theta} \quad (3)$$

Where D is the size of particle, λ= 1.54 Å is the X ray wavelength, θ is the diffraction angle, k=0.89 is the shape factor and β is the FWHM of the peak (full width at half maximum). The crystallization and quality of CNTs was investigated using Micro-Raman spectroscopy (SENTERRA BRUKER, λ= 785nm).

3. RESULTS AND DISCUSSION

3.1. The Effect of Catalyst Composition

In order to examine the effect of catalyst composition on properties of end-product CNTs, different catalyst samples with different mass ratios of catalyst/substrate (Fe-Co/TiO_2) =20-0/80 wt%, 15-5/80 wt%, 10-10/80 wt%, 5-15/80 wt% and 0-20/80 wt% were prepared and used for synthesis of carbon nanotubes at temperature of 700°C. Crystalline structures of the catalysts were characterized by XRD.

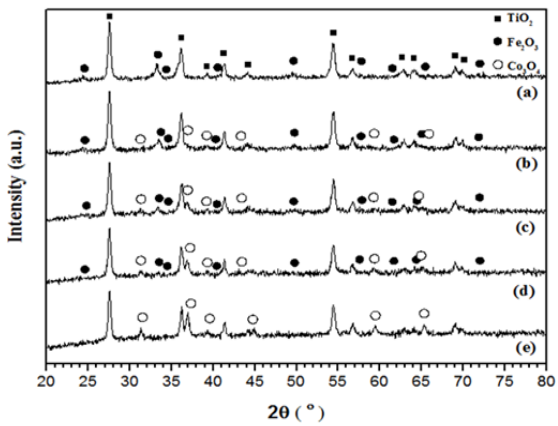

Figure 1. *XRD patterns of the Fe-Co/TiO_2 catalysts with different wt% mass ratios, a) 20-0/80, b) 15-5/80, c) 10-10/80, d) 5-15/80, e) 0-20/80.*

The diffraction patterns are shown in Figure 1. The most intense peaks in Figure 1 correspond to the rutile phase of TiO_2 support which are observed for all compositions of the catalysts at 2θ = 27.5°, 36.1°, 39.2°, 41.3°, 44°, 54.3°, 56.7°, 62.8°, 64°, 69.1° and 70°. Beside the support's peaks, the metal oxides peaks were also observed in the catalysts. The peaks at 2θ = 24.2°, 33.2°, 36.1°, 41°, 49.5°, 57.8°, 62.8°, 64.1° and 72° in Figure 1 (a) to (d) indicate the presence of Fe_2O_3 particles and the peaks at 2θ = 31.3°, 36.9°, 38.5°, 44.9°, 59.4° and 65.3° in Figure 1 (b) to (d), correspond to the Co_3O_4 particles. Furthermore the XRD patterns show that when the amount of metal salts increases the intensity of the corresponding peaks (related metal oxides) increases as well. The approximate sizes of crystallites were calculated using Scherer equation (equation (3)) and shown in Table 1. The approximate sizes of catalyst nanoparticles on different catalyst compositions are nearly similar. It seems that bimetallic composition of Fe and Co lead to smaller particles compared to monometallic ones.

Figure 2 (a) to (e) shows the typical FESEM images of the five catalyst samples. These images exhibit the granular and nanometric structure of different compositions of Fe-Co/TiO_2 catalyst samples. The morphologies of the five compositions of catalysts are nearly similar. The distribution of particles on catalyst-support matrix is relatively uniform and the particles have rather spherical shapes. It seems that bimetallic catalyst samples (Fig.2 (b), (c) and (d)) possess smaller particles and finer

structures compared to monometallic ones (Figure 2(a) and (e)).

Figure 2 (f) to (j) demonstrates the X-ray maps of elemental distributions of the five catalyst samples. For each map a 30×30 micron window of the surface of catalytic powder was investigated. In these images yellow and red points indicate the presence of Fe and Co particles respectively. For clearer appearance background points of Ti particles representing the titania support were removed from the maps. A uniform distribution of catalyst particles was observed on all of the five catalyst compositions. As we expect by increasing the Fe wt% (Co wt%) on catalyst compositions the number of corresponding yellow points (red points) on Xmap patterns increases. For Fe-Co/TiO_2= 10-10/80 wt% catalyst composition nearly the same number of Fe and Co particles was appeared. It seems that a denser distribution of catalyst particles were formed on bimetallic samples compared to monometallic ones.

The carbon yield of the five catalyst compositions and the characteristics of CNTs originated from them were summarized in Table 2.

As shown in this table, the carbon yields of monometallic catalysts (pure Fe and Pure Co samples) were significantly smaller than bimetallic catalysts. This confirms that by combining the two catalyst metals, their catalytic activity could greatly be enhanced and the efficiency of CNTs production and its growth rate significantly be improved [16, 19, 37]. It should be noted that the zero carbon yield of Fe monometallic catalyst (beside the SEM observation of CNT growth, Figure 2(k)), indicates that Fe nanoparticles were not activated on nanometric TiO_2 substrate at 700°C. It seems that a higher growth temperature is needed for the catalytic activation of pure Fe. Therefore it can be concluded that combination of Fe with Co catalyst lowered the activation temperature of Fe catalyst. This result supports the previous finding that binary combination of Fe, Co and Ni with each other or with other elements of transition metals (such as Mo or Pd), enhances the efficiency of CNT production or decreases the synthesis temperature [16, 19, 21, 26, 28, 37, 38]. Figure 2(k) to (o) shows the FESEM images of the as-synthesized carbon deposits on the five catalyst compositions which indicates that except for pure Fe, significant growth of CNTs on other compositions of the catalysts were obtained. Using these SEM images, statistical diameter distributions of the grown CNTs were obtained and the

Table 1. *Approximate sizes of metal oxide particles produced on different catalyst samples.*

Mass ratio of Fe-Co/TiO_2	Metal oxide	Particle size (nm)
20-0/80	Fe_2O_3	16
15-5/80	Fe_2O_3	11
	Co_3O_4	8
10-10/80	Fe_2O_3	16
	Co_3O_4	11
5-15/80	Fe_2O_3	10
	Co_3O_4	10
0-20/80	Co_3O_4	14

Table 2. *The carbon yield percentage and characteristics of grown CNTs on different catalyst samples.*

Mass ratio of Fe-Co/TiO_2	Carbon yield (%)	Average diameter of grown CNTs (nm)	Average growth rate (mg/min)	I_G/I_D
20-0/80	0	-	-	-
15-5/80	300	41	10	0.50
10-10/80	340	34	11.3	0.51
5-15/80	340	42	11.3	0.54
0-20/80	120	38	4	0.54

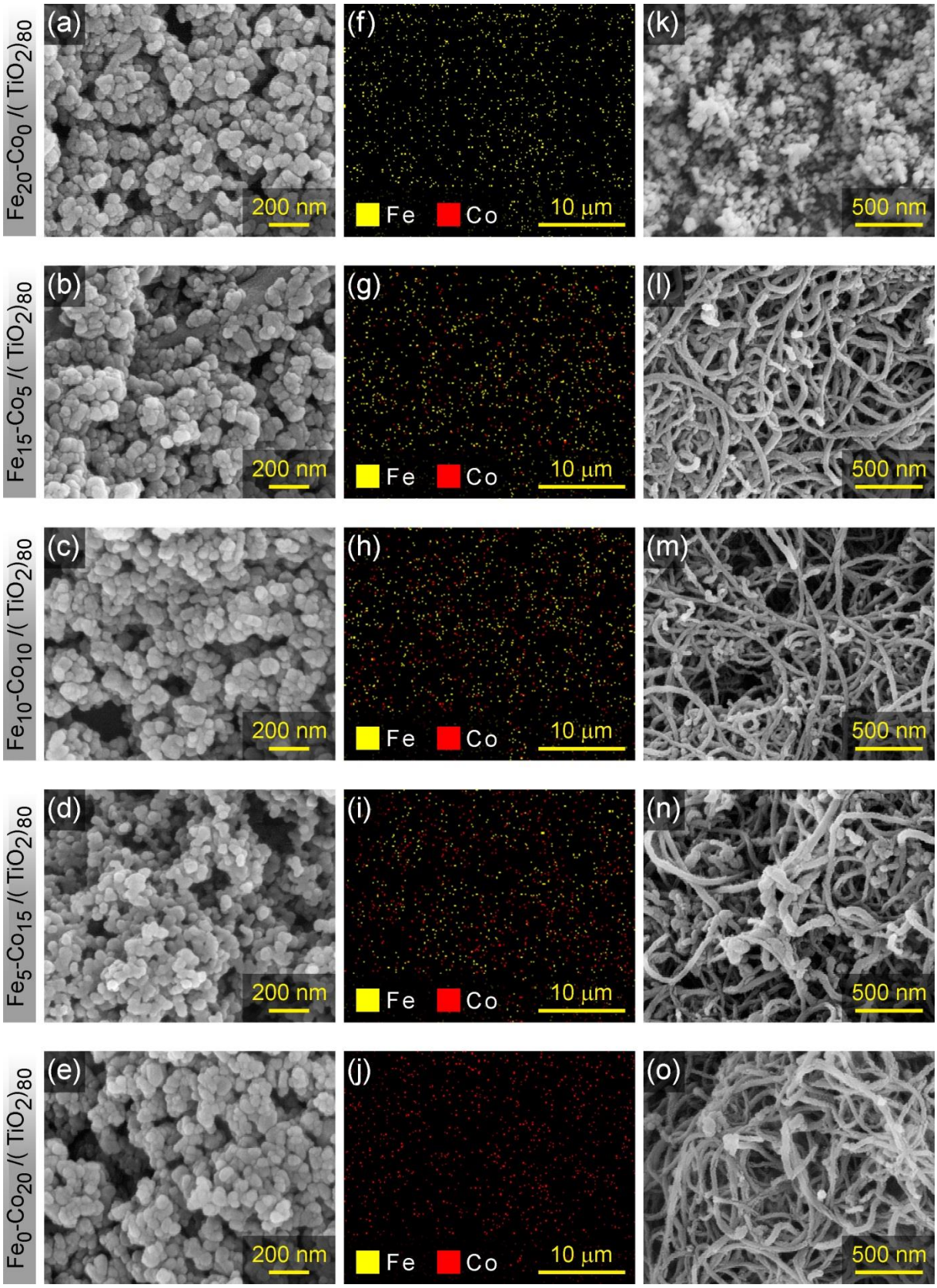

Figure 2. *FESEM images of catalyst basis with wt% of Fe-Co/TiO_2 : a) 20-0/80, b) 15-5/80, c) 10-10/80, d) 5-15/80 and e) 0-20/80. Xmap images of catalyst basis with wt% of Fe-Co/TiO_2 : f) 20-0/80, g) 15-5/80, h) 10-10/80, i) 5-15/80 and j) 0-20/80. FESEM images of grown CNTs on different catalysts basis with wt% of Fe-Co/TiO_2 : k) 20-0/80, l) 15-5/80, m) 10-10/80, n) 5-15/80 and o) 0-20/80.*

average diameters of the nanotubes were calculated and presented in Table 2. Our observations show that the best catalyst composition for CNT production is Fe-Co/TiO_2=10-10/80 wt%, because this composition led to maximum abundance of CNTs with minimum average diameter. Furthermore, it can be concluded that the addition of Fe particles to pure Co catalyst has beneficial result. At the critical mass ratio of Fe-Co/ TiO_2=10-10/80 wt%, the best catalytic activity is obtained. After this critical point, addition of more Fe content may lead to destructive results.

In order to investigate the crystallinity of the grown CNTs, Raman spectroscopy was executed. Figure 3 represents the Raman spectra of the grown CNTs on different catalyst samples. The Raman band appearing in 1500-1605 cm^{-1} region of the wave number is ascribed to G band (graphite band) and the one appearing in 1250-1450 cm^{-1} spectral region is known as D band (disorder-induced band). The G band is assigned to C-C vibration frequency of the carbon material with sp^2 orbital structure and the D band contributed to disorder-induced vibration of C-C band [41]. According to Figure 3, two peaks corresponding to the D and G bands of MWCNTs appeared in each spectrum. The intensity ratio of G to D band, I_G/I_D is known as a rough measure for the quality of produced CNTs. This parameter was calculated from Raman analysis and shown in Table 2. Considering this Table, it can be concluded that in bimetallic catalysts with increasing Co content, the quality and order of crystallinity of grown CNTs were slightly improved. This result confirms the previous reports that the catalytic activity of iron nanoparticles is higher than cobalt ones. However the quality and order of crystallinity of the nanotubes in the vicinity of Fe catalyst is lower than Co [16].

3.2. The Effect of Growth Temperature

In order to acquire the optimum temperature for the growth of carbon nanotubes, different experiments were performed on Fe-Co/TiO_2 catalysts with mass ratio of 10-10/80 wt%, at different temperatures of 650, 700, 750 and 800°C. Figure 4 shows the typical FESEM images of the grown CNTs at different growth temperatures. The appearance of filamentous carbon nanomaterial is an indication of carbon nanotubes formation. Except of 800°C, a dense, massive and relatively uniform growth of CNTs at examined temperatures was achieved. By means of FESEM images, the diameter distribution histograms of grown CNTs were obtained and carbon yield, average growth rate and the average diameters of CNTs were calculated and shown in Table 3. The average diameters of grown CNTs at 650, 700, 750°C are close to each other, however it increases dramatically at 800°C. The minimum average diameter of CNTs was achieved at 650°C and the highest yield of CNTs' production was obtained at 700°C. Considering Figure 4 and Table 3 it can be concluded that increasing the growth temperature leads to an increasing trend in the diameter of the nanotubes, average growth rate, and the amount of contaminations in the samples

Table 3. *The carbon yield percentage and characteristics of grown CNTs at different growth temperatures.*

Synthesis Temperature (°C)	Carbon yield (%)	Average diameter of grown CNTs (nm)	Average growth rate (mg/min)	I_G/I_D
650	280	32	9.3	0.49
700	340	34	11.3	0.51
750	340	35	11.3	0.55
800	220	52	7.3	0.57

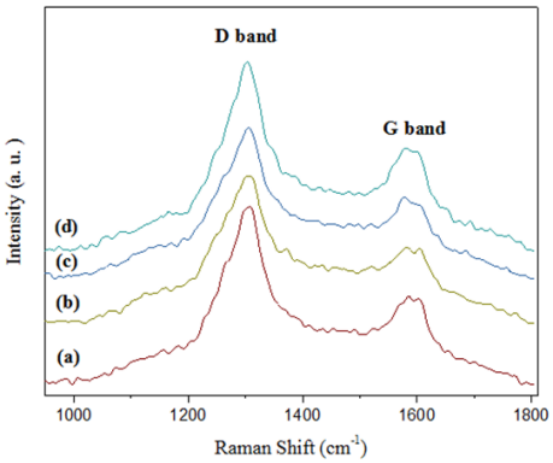

Figure 3. *Raman spectrum of the grown CNTs at different wt% mass ratios of Fe-Co/TiO_2, a) 15-5/80, b) 10-10/80, c) 5-15/80 and d) 0-20/80.*

along with a reduction in the length and density of CNTs. The CNTs with larger diameter and lower density are grown by raising the growth temperature. Increasing the growth temperature may lead to agglomeration of catalyst particles, so at higher temperature, larger catalyst particles can be formed. It is generally accepted that the sizes of catalyst particles usually determine the diameters of CNTs in CVD approach [16, 19, 42]. On the other hand, increasing the growth temperature, results in more impurities in the final product which may also relate to formation of larger catalyst particles at higher temperatures. These larger catalyst particles have lower catalytic activities which may cause to formation of amorphous carbon [27]. Figure 5 represents Raman spectra of the grown CNTs at different growth temperatures. The I_G/I_D ratios of the grown CNTs were calculated using these spectra and shown in Table 3. Raman spectroscopy indicated that increasing the growth temperature gradually improves the quality of produced CNTs, which is in accordance with the finding of other researchers [27, 43].

4. CONCLUSIONS

In summary, we have successfully grown CNTs on a wet impregnation prepared mixture of iron and cobalt nanoparticles supported on TiO_2 substrate from decomposing of acetylene by TCVD in the temperature range of 650-800°C. It was observed that the growth rate, diameter and crystallinity of CNTs can be controlled by adjusting the growth temperature. With increasing the temperature from 650°C to 800°C, the growth rate, average diameter, and the amount of impurities increase along with reduction in the length and

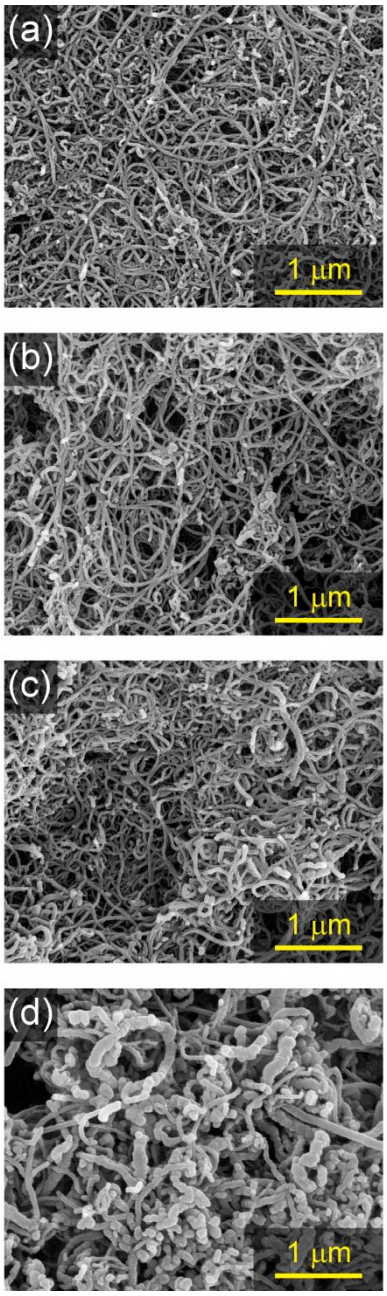

Figure 4. *SEM images of the CNTs grown on Fe-Co/TiO_2=10-10/80 wt% catalyst at a) 650°C, b) 700°C, c) 750°C, d) 800°C.*

density of CNTs. In addition, CNTs were synthesized on different composition of monometallic and bimetallic Fe and Co catalysts which further proves that the carbon yield of the catalyst and its activity, the average diameter of end-product CNTs, and the density of the growth are significantly influenced by the composition of the catalyst. No growth of CNTs on titania supported pure Fe catalyst was achieved. The growth on binary combination of Fe and Co was much more successful than monometallic Co catalyst. The best catalytic activity and the most favourable growth of CNTs was obtained on the catalyst-support composition of Fe-Co/TiO_2 = 10-10/80 %wt.

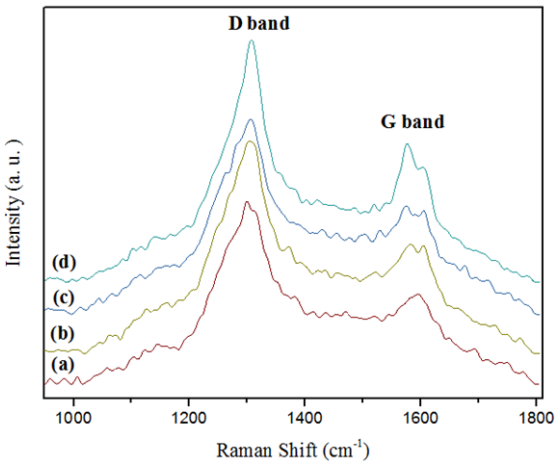

Figure 5. *Raman spectrum of the grown CNTs on Fe-Co/TiO_2=10-10/80 wt% catalyst at a) 650°C, b) 700°C, c) 750°C, d) 800°C.*

REFERENCES

1. Iijima, S., (1991). "Helical microtubules of graphitic carbon", *nature*, 354: 56-58.
2. Harris, P. J. F., Harris, P. J. F., (2009). "*Carbon Nanotube Science: Synthesis, Properties and Applications*", Cambridge University Press.
3. Popov, V. N., (2004). "Carbon nanotubes: Properties and application", *Mater. Sci. Eng., R, 43*: 61-102.
4. De Volder, M. F. L., Tawfick, S. H., Baughman, R. H., Hart, A. J., (2013). "Carbon nanotubes: Present and future commercial applications", *Science*, 339: 535-539.
5. Zhang, Q., (2012). "*Carbon Nanotubes and Their Applications*", CRC Press.
6. Tan, C. W., Tan, K. H., Ong, Y. T., Mohamed, A. R., Zein, S. H. S., Tan, S. H., (2012). "Energy and environmental applications of carbon nanotubes", *Environ. Chem. Lett.*, 10: 265-273.
7. Verma, P., Saini, P., Malik, R. S., Choudhary, V., (2015). "Excellent electromagnetic interference shielding and mechanical properties of high loading carbon-nanotubes/polymer composites designed using melt recirculation equipped twin-screw extruder", *Carbon*, 89: 308-317.
8. Cheng, Y., Xu, C., Jia, L., Gale, J. D., Zhang, L., Liu, C., Shen, P. K., Jiang, S. P., (2015). "Pristine carbon nanotubes as non-metal electrocatalysts for oxygen evolution reaction of water splitting", *Appl. Catal., B*, 163: 96-104.
9. Alsawat, M., Altalhi, T., Kumeria, T., Santos, A., Losic, D., (2015). "Carbon nanotube-nanoporous anodic alumina composite membranes with controllable inner diameters and surface chemistry: Influence on molecular transport and chemical selectivity", *Carbon*, 93: 681-692.
10. Hou, P.-X., Liu, C., Cheng, H.-M., (2008). "Purification of carbon nanotubes", *Carbon*, 46: 2003-2025.
11. Hamidi Malayeri, F., Sohrabi, M. R., Ghourchian, H., (2012). "Magnetic multi-walled carbon nanotube as an adsorbent for toluidine blue O removal from aqueous solution", *Int. J. Nanosci. Nanotechnol.*, 8: 79-86.
12. Kolangikhah, M., Maghrebi, M., Ghazvini, K., Farhadian, N., (2012). "Separation of salmonella typhimurium bacteria from water using MWCNTs arrays", *Int. J. Nanosci. Nanotechnol.*, 8: 3-10.
13. Arora, N., Sharma, N., (2014). "Arc discharge synthesis of carbon nanotubes: Comprehensive review", *Diamond Relat. Mater.*, 50: 135-150.
14. Chrzanowska, J., Hoffman, J., Małolepszy, A., Mazurkiewicz, M., Kowalewski, T. A., Szymanski, Z., Stobinski, L., (2015). "Synthesis of carbon nanotubes by the laser ablation method: Effect of laser wavelength", *Phys. Status Solidi B*, 252: 1860-1867.
15. Jourdain, V., Bichara, C., (2013). "Current understanding of the growth of carbon nanotubes in catalytic chemical vapour deposition", *Carbon*, 58: 2-39.
16. Dupuis, A.-C., (2005). "The catalyst in the CCVD of carbon nanotubes-a review", *Prog. Mater Sci.*, 50: 929-961.
17. Yu, Z., Chen, D., Tøtdal, B., Holmen, A., (2005). "Effect of catalyst preparation on the carbon nanotube growth rate", *Catal. Today*, 100: 261-267.
18. Mubarak, N., Abdullah, E., Jayakumar, N., Sahu, J., (2014). "An overview on methods for the production of carbon nanotubes", *J. Ind. Eng. Chem.*, 20: 1186-1197.

19. Kumar, M., Ando, Y., (2010). "Chemical vapor deposition of carbon nanotubes: a review on growth mechanism and mass production", *J. Nanosci. Nanotechnol.*, 10: 3739-3758.
20. Zhang, Q., Huang, J. Q., Zhao, M. Q., Qian, W. Z., Wei, F., (2011). "Carbon nanotube mass production: principles and processes", *ChemSusChem., 4*: 864-889.
21. Lobiak, E., Shlyakhova, E., Bulusheva, L., Plyusnin, P., Shubin, Y. V., Okotrub, A., (2015). "Ni–Mo and Co–Mo alloy nanoparticles for catalytic chemical vapor deposition synthesis of carbon nanotubes", *J. Alloys Compd.*, 621: 351-356.
22. Takagi, D., Hibino, H., Suzuki, S., Kobayashi, Y., Homma, Y., (2007). "Carbon nanotube growth from semiconductor nanoparticles", *Nano Lett., 7*: 2272-2275.
23. Tan, L.-L., Ong, W.-J., Chai, S.-P., Mohamed, A. R., (2013). "Growth of carbon nanotubes over non-metallic based catalysts: A review on the recent developments", *Catal. Today*, 217: 1-12.
24. Chiang, W.-H., Sankaran, R. M., (2009). "Linking catalyst composition to chirality distributions of as-grown single-walled carbon nanotubes by tuning NixFe1− x nanoparticles", *Nat. Mater., 8*: 882-886.
25. Pasha, M. A., Shafiekhani, A., Vesaghi, M., (2009). "Hot filament CVD of Fe–Cr catalyst for thermal CVD carbon nanotube growth from liquid petroleum gas", *Appl. Surf. Sci.*, 256: 1365-1371.
26. Mortazavi, S., Reyhani, A., (2008). "The effect of Pd addition to Fe as catalysts on growth of carbon nanotubes by TCVD method", *Appl. Surf. Sci.*, 254: 6416-6421.
27. Pasha, M. A., Poursalehi, R., Vesaghi, M., Shafiekhani, A., (2010). "The effect of temperature on the TCVD growth of CNTs from LPG over Pd nanoparticles prepared by laser ablation", *Phys. B*, 405: 3468-3474.
28. Shah, K. A., Tali, B. A., (2016). "Synthesis of carbon nanotubes by catalytic chemical vapour deposition: A review on carbon sources, catalysts and substrates", *Mater. Sci. Semicond. Process*, 41: 67-82.
29. Tsoufis, T., Xidas, P., Jankovic, L., Gournis, D., Saranti, A., Bakas, T., Karakassides, M. A., (2007). "Catalytic production of carbon nanotubes over Fe-Ni bimetallic catalysts supported on MgO", *Diamond Relat. Mater.*, 16: 155-160.
30. Huang, Z., Wang, D., Wen, J., Sennett, M., Gibson, H., Ren, Z., (2002). "Effect of nickel, iron and cobalt on growth of aligned carbon nanotubes", *Appl. Phys. A*, 74: 387-391.
31. Harutyunyan, A. R., Pradhan, B. K., Kim, U., Chen, G., Eklund, P., (2002). "CVD synthesis of single wall carbon nanotubes under "soft" conditions", *Nano Lett., 2*: 525-530.
32. Kichambare, P. D., Qian, D., Dickey, E. C., Grimes, C. A., (2002). "Thin film metallic catalyst coatings for the growth of multiwalled carbon nanotubes by pyrolysis of xylene", *Carbon*, 40: 1903-1909.
33. Alvarez, W. E., Kitiyanan, B., Borgna, A., Resasco, D. E., (2001). "Synergism of Co and Mo in the catalytic production of single-wall carbon nanotubes by decomposition of CO", *Carbon*, 39: 547-558.
34. Hernadi, K., Fonseca, A., Nagy, J. B., Siska, A., Kiricsi, I., (2000). "Production of nanotubes by the catalytic decomposition of different carbon-containing compounds", *Appl. Catal. A*, 199: 245-255.
35. Masoumi, M., Mehrnia, M. R., Montazer-Rahmati, M. M., Rashidi, A. M., (2010). "Templated growth of carbon nanotubes on nickel loaded mesoporous MCM-41 and MCM-48 molecular sieves", *Int. J. Nanosci. Nanotechnol.*, 6: 88-96.
36. Jabari Seresht, R., Jahanshahi, M., Raoof, J., Khorram, M., (2009). "Optimization of experimental conditions for fabrication of carbon nanotubes based on taguchi robust design method", *Int. J. Nanosci. Nanotechnol.*, 5: 9-18.
37. Kathyayini, H., Nagaraju, N., Fonseca, A., Nagy, J., (2004). "Catalytic activity of Fe, Co and Fe/Co supported on Ca and Mg oxides, hydroxides and carbonates in the synthesis of carbon nanotubes", *J. Mol. Catal. A: Chem.*, 223: 129-136.
38. Pudukudy, M., Yaakob, Z., Akmal, Z. S., (2015). "Direct decomposition of methane over SBA-15 supported Ni, Co and Fe based bimetallic catalysts", *Appl. Surf. Sci.*, 330: 418-430.
39. Chen, H., Wang, L., (2014). "Nanostructure sensitization of transition metal oxides for visible-light photocatalysis", *Beilstein J. Nanotechnol.*, 5: 696-710.
40. Soroodan Miandoab, E., Fatemi, S., (2014). "Upgrading TiO_2 photoactivity under visible light by synthesis of MWCNT/TiO_2 nanocomposite", *Int. J. Nanosci. Nanotechnol.*, 11: 1-12.
41. Dresselhaus, M. S., Dresselhaus, G., Saito, R., Jorio, A., (2005). "Raman spectroscopy of carbon nanotubes", *Phys. Rep.*, 409: 47-99.
42. Lee, C. J., Park, J., Huh, Y., Lee, J. Y., (2001). "Temperature effect on the growth of carbon nanotubes using thermal chemical vapor deposition", *Chem. Phys. Lett.*, 343: 33-38.
43. Kim, K.-E., Kim, K.-J., Jung, W. S., Bae, S. Y., Park, J., Choi, J., Choo, J., (2005). "Investigation on the temperature-dependent growth rate of carbon nanotubes using chemical vapor deposition of ferrocene and acetylene", *Chem. Phys. Lett.*, 401: 459-464.